BIOMETRIC METHODOLOGY

Distribution-free estimation of local growth rates around interval censored anchoring events†

Chenghao Chu and Ying Zhang and Wanzhu Tu

Department of Biostatistics, Indiana University Fairbanks School of Public Health Indiana, University School of Medicine, Indianapolis, Indiana 46202, U.S.A.

**email*: wtu1@iu.edu

This paper has been submitted for consideration for publication in *Biometrics*

Additional Supporting Information may be found in the online version of this article.

Received 20 March 2018; Revised 8 November 2018; Accepted 6 December 2018
Biometrics

DOI 10.1111/biom.13015

This is the author's manuscript of the article published in final edited form as:

Chu, C., Zhang, Y., & Tu, W. (2019). Distribution-free estimation of local growth rates around interval censored anchoring events. Biometrics, 0(ja). https://doi.org/10.1111/biom.13015

Summary: Biological processes are usually defined on timelines that are anchored by specific events. For example, cancer growth is typically measured by the change in tumor size from the time of oncogenesis. In the absence of such anchoring events, longitudinal assessments of the outcome lose their temporal reference. In this paper, we considered the estimation of local change rates in the outcomes when the anchoring events are interval-censored. Viewing the subject-specific anchoring event times as random variables from an unspecified distribution, we proposed a distribution-free estimation method for the local growth rates around the unobserved anchoring events. We expressed the rate parameters as stochastic functionals of the anchoring time distribution and showed that under mild regularity conditions, consistent and asymptotically normal estimates of the rate parameters could be achieved, with a $\sqrt{n}$ convergence rate. We conducted a carefully designed simulation study to evaluate the finite sample performance of the method. To motivate and illustrate the use of the proposed method, we estimated the skeletal growth rates of male and female adolescents, before and after the unobserved pubertal growth spurt (PGS) times. This article is protected by copyright. All rights reserved

Key words: Empirical process; Interval censoring; Nonparametric maximum likelihood; Pubertal growth.

1. Introduction

In biomedical research, investigators are often interested in estimating the change rates of specific outcomes around events of clinical significance. For example, oncologists are interested in the rates of neoplastic growth following the initial tumorigenesis or subsequent tumor recurrence (Carter et al., 1989; Fournier et al., 1980; Spratt et al., 1993). Human growth researchers are interested in rates of skeletal changes before and after pubertal growth spurt (PGS), the time at which a child's height increase reaches its maximum velocity (Tanner and Whitehouse, 1976). In these applications, tumorigenesis/recurrence and PGS function respectively as the anchoring points of cancer and skeletal growth, while tumor size and skeletal measurements are the study outcomes of primary interest. In these studies, the anchoring event plays a critical role in placing the outcome assessments into the observational timeline of an individual subject. Without knowing the time of the anchoring event time T_i, all observations $\mathbf{Y}_i$ from the individual would lose their temporal reference. In pubertal growth research, unless we know the timing of PGS, it would not be possible to determine the rates of skeletal changes around PGS.

Short of precisely observed anchoring event time, investigators sometimes are able to determine the interval that covers T_i, i.e., $U_i < T_i \leqslant V_i$. Clinicians, for example, can usually determine the intervals of tumorigenesis or cancer recurrence with a reasonable accuracy. Similarly, human growth researchers are often able to specify the age range that contains the PGS. In these situations, the anchoring events can be viewed as interval-censored. Here the term "interval censoring" is used to refer to situations where the *anchoring events* are not precisely observed. In survival analysis, the same term is used to indicate situations where the *main events* are confined to certain intervals (Zhang and Sun, 2010). The problem that we are studying here is also different from the change-point problems, where the focus is to determine the times at which changes occur to the outcome Y (Lee, 2010). Herein,

we exclusively focus on the situations where the events anchoring the study timeline are interval-censored.

An intuitive solution to the problem is to impute T_i. In the human growth literature, various parametric and nonparametric models are available for the depiction of individual human growth curves (Gasser et al., 1984; Preece and Baines, 1978). From the fitted subject-specific curves, it is often possible to impute the PGS time T_i for a given subject, e.g., by maximizing the first derivative functions of the fitted height curves (Tu et al., 2009). However, from a population perspective, the anchoring event time T_i is a random quantity that varies from subject to subject. Imputing or predicting a random quantity accurately and reliably tends to be a difficult, if not impossible task. More important, many of the imputation methods lack proper accommodation of the uncertainty associated with the estimate $\hat{T}_i$, and thus are prone to produce questionable inferences. An alternative approach is to conduct a joint modeling analysis by assuming a parametric distribution for T (Robinson et al., 2010; van den Hout et al., 2013). Such assumptions, however, are impossible to verify, and misspecified distributions could lead to biased estimation.

In this paper, we put forward a distribution-free solution to the problem: We first obtain a nonparametric maximum likelihood estimator for $\hat{F}$, the cumulative distribution function (CDF) of T. We then embed the estimated CDF $\hat{F}$ into the least-square estimating equations for $\boldsymbol{\theta}$, from which we ascertain the estimates $\hat{\boldsymbol{\theta}}$. The final estimators of interest are expressed as smooth functionals of $\hat{F}$. Because the method does not assume a parametric distribution for the anchoring event time T, it is expected to produce more robust estimates.

This research extends beyond the recent work of Zhang et al. (2016), who developed a robust nonparametric estimator for monotone regression functions, and showed that their estimator was consistent. The rate of convergence of their estimator, however, is not sufficiently fast to ensure asymptotic normality. As a result, their method does not lend itself

to large sample inference. Using the empirical process theory (Kosorok, 2008), we showed that the estimators proposed in this paper were consistent and asymptotically normal. We provided both theoretical and numerical evidence in support of the claim. For narrative convenience, we described the estimation in the context of skeletal growth.

2. Distribution-free estimation of local rates

Suppose there are n independent subjects. For the ith subject, $i = 1, 2, \ldots, n$, the anchoring event time T_i is known to occur in interval $(U_i, V_i]$, i.e., $U_i < T_i \leqslant V_i$, where U_i and V_i come from a sequence of screening times generated by a process independent of T_i. The outcome of interest Y is assessed at the two end points of the censoring interval, denoted respectively as Y_{U_i} and Y_{V_i}. For convenience, we write the observed data from the ith subject as $W_i = (U_i, V_i, Y_{U_i}, Y_{V_i})$, and we assume that $W_1, W_2, \cdots, W_n$ form an independent and identically distributed sample.

The goal of the analysis is to estimate the mean change rates in Y, immediately before and after the anchoring point T, herein referred to as the local rates. In studies of human growth, these local rates, collectively, depict the skeletal changes at the time of PGS.

Because the interest is confined to the neighborhood around PGS, we limit the observations to the skeletal measures at the two ends of the interval. To analyze, we write a simple piecewise linear regression model with a latent random anchoring event time T

$$\begin{cases} E(Y_U|T) = \lambda + \alpha(U - T), \\ E(Y_V|T) = \lambda + \beta(V - T), \end{cases} \tag{1}$$

where λ is the population average value of the response variable Y at time T; α and β are the respective mean pre- and post-anchoring event rates of change in Y; and U and V are random observation times bracketing T, they are assumed to follow an unspecified joint distribution $H(u, v)$. Let $\epsilon_U = Y_U - E(Y_U|T, U)$ and $\epsilon_V = Y_V - E(Y_V|T, V)$ be the random errors that

follow an unknown joint distribution $\psi(\cdot,\cdot)$. It then follows that $E(\epsilon_U) = E(\epsilon_V) = 0$. We also assume $\int \psi^2(\epsilon_U, \epsilon_V) d\epsilon_U d\epsilon_V < \infty$.

An implicit assumption is that the local growth rates are adequately depicted by this linear model. In the human growth application, growth curves are known to be smooth and the interval that brackets the PGS is relatively tight. An advantage for adopting a linear model is that both pre and post-anchoring event rates are explicitly specified, as α and β in (1).

More generally, nonlinear functions or functions with higher order terms can be incorporated in the following structure:

$$\begin{cases} E(Y_U|T) = \boldsymbol{\lambda}^t \cdot \mathbf{Z} + \boldsymbol{\alpha}^t \cdot \boldsymbol{B}(U-T), \\ E(Y_V|T) = \boldsymbol{\lambda}^t \cdot \mathbf{Z} + \boldsymbol{\beta}^t \cdot \boldsymbol{B}(V-T), \end{cases} \tag{2}$$

where $\mathbf{Z}$ is a vector of time-invariant covariates, and $\boldsymbol{B}(t) = \big(b_1(t), \cdots, b_q(t)\big)^T$ is a vector of functions satisfying the regularity conditions stated in Section 3.

Despite the relatively simple modeling structure, fitting Models (1) and (2) without knowing the anchoring event time T remains a challenge. For convenience, we let $\boldsymbol{\theta}_0$ be the true parameter vector $(\lambda_0, \alpha_0, \beta_0)^t$ in Model (1), or more generally $(\boldsymbol{\lambda}_0, \boldsymbol{\alpha}_0, \boldsymbol{\beta}_0)^t$ in Model (2).

Let F_0 be the true distribution of T. We note that the true parameter $(\boldsymbol{\theta}_0, F_0)$ minimizes the deterministic functional

$$\mathbb{M}(\boldsymbol{\theta}, F) = E_{Y_U, Y_V, U, V}\Big\{\big(Y_U - E_{F, U<T\leqslant V} Y_U\big)^2 + \big(Y_V - E_{F, U<T\leqslant V} Y_V\big)^2\Big\},$$

where $\boldsymbol{\theta} = (\lambda, \alpha, \beta)^t$ contains parameters in Model (1), F covers all CDFs, and $E_{F, U<T\leqslant V}(\cdot)$ is the conditional expectation given $U < T \leqslant V$ under distribution F.

Intuitively, one could estimate $(\boldsymbol{\theta}_0, F_0)$ by minimizing the corresponding stochastic functional

$$\mathbb{M}_n(\boldsymbol{\theta}, F) = \sum_{i=1}^{n} \Big\{\big(Y_{U_i} - E_{F, U_i<T_i\leqslant V_i} Y_{U_i}\big)^2 + \big(Y_{V_i} - E_{F, U_i<T_i\leqslant V_i} Y_{V_i}\big)^2\Big\}.$$

But minimizing $\mathbb{M}_n(\boldsymbol{\theta}, F)$ jointly over the entire ranges of $\boldsymbol{\theta}$ and F is a computationally daunting task. To resolve, we take a two-step procedure:

In Step 1, we obtain $\hat{F}_n$, a nonparametric maximum likelihood estimator (NPMLE) of F_0 (Groeneboom and Wellner, 1992). By definition, $\hat{F}_n$ is the unique solution that maximizes nonparametric likelihood function

$$\hat{F}_n = \arg\max_{F\in\mathcal{F}} \prod_{i=1}^{n} \Big\{F(V_i) - F(U_i)\Big\},$$

where $\mathcal{F}$ is the class of all stepwise CDFs that do not have jumps outside of the set $\{U_1, \cdots, U_n, V_1, \cdots, V_n\}$. Estimated distribution $\hat{F}_n$ can be ascertained by using an efficient numerical algorithm, as described by Zhang and Jamshidian (2004).

In Step 2, we obtain $\hat{\boldsymbol{\theta}}_n = (\hat{\lambda}_n, \hat{\alpha}_n, \hat{\beta}_n)^t$, which is an M-estimator of $\boldsymbol{\theta}_0$, by minimizing the plug-in stochastic objective function

$$\mathbb{M}_n(\boldsymbol{\theta}, \hat{F}_n) = \sum_{i=1}^{n} \Big\{\big(Y_{U_i} - E_{\hat{F}_n, U_i<T_i\leqslant V_i} Y_{U_i}\big)^2 + \big(Y_{V_i} - E_{\hat{F}_n, U_i<T_i\leqslant V_i} Y_{V_i}\big)^2\Big\},$$

where $E_{\hat{F}_n, U_i, V_i}(\cdot)$ is the conditional expectation given $U_i < T_i \leqslant V_i$, under the estimated CDF $\hat{F}_n$.

Under Model (2), we have $E_{\hat{F}_n, U_i<T_i\leqslant V_i} Y_{U_i} = \boldsymbol{\lambda}^t \cdot \mathbf{Z}_i + \boldsymbol{\alpha}^t \cdot E_{\hat{F}_n, U_i<T_i\leqslant V_i} \boldsymbol{B}(U_i - T_i)$ and $E_{\hat{F}_n, U_i<T_i\leqslant V_i} Y_{V_i} = \boldsymbol{\lambda}^t \cdot \mathbf{Z}_i + \boldsymbol{\alpha}^t \cdot E_{\hat{F}_n, U_i<T_i\leqslant V_i} \boldsymbol{B}(V_i - T_i)$. Letting $s_1 < s_2 < \cdots < s_k$ be the set of time points at which $\hat{F}_n$ jumps, and letting $\hat{p}_i = \hat{F}_n(s_i) - \hat{F}_n(s_i-)$ be the magnitude of the jump at s_i, we can calculate the expectation vector $E_{\hat{F}_n, U_i<T_i\leqslant V_i} \boldsymbol{B}(U_i - T_i)$ as

$$E_{\hat{F}_n, U_i<T\leqslant V_i} \boldsymbol{B}(U_i - T_i) = \sum_{U_i<s_j\leqslant V_i} \hat{p}_j \boldsymbol{B}(U_i - s_j) \Big/ \sum_{U_i<s_j\leqslant V_i} \hat{p}_j \,.$$

Similarly, the expectation vector $E_{\hat{F}_n, U_i<T_i\leqslant V_i} \boldsymbol{B}(V_i - T_i)$ can be calculated.

An immediate benefit of taking the two-step approach is that the parameter estimator $\hat{\boldsymbol{\theta}}_n$ has a closed-form solution. Let

$$\boldsymbol{X}_i(\hat{F}_n) = \begin{pmatrix} \mathbf{Z}_i^t & E_{\hat{F}_n, U_i<T_i\leqslant V_i} \boldsymbol{B}(U_i - T_i)^t & \mathbf{0} \\ \mathbf{Z}_i^t & \mathbf{0} & E_{\hat{F}_n, U_i<T_i\leqslant V_i} \boldsymbol{B}(V_i - T_i)^t \end{pmatrix}, \quad \boldsymbol{Y}_i = \begin{pmatrix} Y_{U_i} \\ Y_{V_i} \end{pmatrix}.$$

The proposed estimator is essentially the least-square estimator $\hat{\boldsymbol{\theta}}_n$ that minimizes

$$\mathbb{M}_n(\boldsymbol{\theta}, \hat{F}_n) = \sum_{i=1}^{n} \Big\{\boldsymbol{Y}_i - \boldsymbol{X}_i(\hat{F}_n)\boldsymbol{\theta}\Big\}^t \Big\{\boldsymbol{Y}_i - \boldsymbol{X}_i(\hat{F}_n)\boldsymbol{\theta}\Big\}.$$

It then follows that the minimizer $\hat{\boldsymbol{\theta}}_n$ has a closed-form solution, given by

$$\hat{\boldsymbol{\theta}}_n = \Big\{ \sum_{i=1}^{n} \boldsymbol{X}_i(\hat{F}_n)^t \boldsymbol{X}_i(\hat{F}_n) \Big\}^{-1} \Big\{ \sum_{i=1}^{n} \boldsymbol{X}_i(\hat{F}_n)^t \boldsymbol{Y}_i \Big\}.$$

Since $\hat{\boldsymbol{\theta}}_n$ is a stochastic functional of $\hat{F}_n$, we write it as $\mathbb{Q}_n(\hat{F}_n)$.

3. Asymptotic properties of $\hat{\boldsymbol{\theta}}_n$

For inference, we examine the asymptotic behavior of the stochastic functional estimator $\hat{\boldsymbol{\theta}}_n = \mathbb{Q}_n(\hat{F}_n)$, which is by definition an M-estimator of the stochastic objective function $\mathbb{M}_n(\boldsymbol{\theta}; \hat{F}_n)$.

If F_0, the true CDF of the anchoring event times is known, the asymptotic properties of $\tilde{\boldsymbol{\theta}}_n = \mathbb{Q}_n(F_0)$, an M-estimator of $\mathbb{M}_n(\boldsymbol{\theta}; F_0)$, will follow directly from the standard M-estimation theory for parametric models (Huber, 2011).

When F_0 is unknown, as in the current setting, we first note that its NPMLE $\hat{F}_n$ converges to F_0 at a rate of $n^{\frac{1}{3}}$ (Groeneboom and Wellner, 1992). In such a situation, development of the asymptotic properties of $\hat{\boldsymbol{\theta}}_n = \mathbb{Q}_n(\hat{F}_n)$, the M-estimator for $\mathbb{M}_n(\boldsymbol{\theta}, \hat{F}_n)$, is technically more challenging with the use of empirical process theory (Kosorok, 2007).

In this current research, we do not have directly observed T, nor do we know its distribution F_0. We do, however, assume that the boundaries of the censoring interval $(U, V]$ can be reliably identified. In the context of the pubertal growth application, U and V are the visit times that flank the peak growth interval, which can be identified by comparing the rates of height increase between all consecutive visits. So technically this is a scenario of case-K censoring, as described by Geskus and Groeneboom (1995, 1999). As the authors observed in their 1999 report, the only times that are relevant to the estimation of F_0 are the ones that immediately bracket the anchoring event time T. Therefore, we focus on the case-2 situation, regardless of how the bracketing interval is identified.

With the censoring intervals identified, we lay out the regularity conditions that are necessary for the asymptotic properties of $\hat{\boldsymbol{\theta}}_n$:

C1: The sequence of screening times are jointly independent of the true event time T. The boundaries U and V of the censoring interval $(U, V]$ are the adjacent screening times that bracket T.

C2: There exist constants $\tau_1 < \tau_2 < \infty$ such that the support of the density function f_T of the anchoring event time T is contained in $[\tau_1, \tau_2]$. The support of F_0, the CDF of T, is included in the union of the supports of the CDFs of U and V.

C3: There exists a constant c such that the probability $P\big[F_0(V) - F_0(U) > c\big] = 1$.

C4: The sum of density functions of U and V, $f_U + f_V$, is strictly positive over $[\tau_1, \tau_2]$.

C5: The joint density function of (U, T, V) is twice differentiable over $[\tau_1, \tau_2]$. In particular, f_U and f_V are differentiable and uniformly bounded over $[\tau_1, \tau_2]$.

C6: The density function f_T is twice differentiable over $[\tau_1, \tau_2]$.

C7: Each component function $b_i(t)$ of $\boldsymbol{B}(t) = \big(b_1(t), \cdots, b_q(t)\big)^T$ is twice differentiable over $[\tau_1 - \tau_2, 0]$, twice differentiable over $[0, \tau_2 - \tau_1]$, and $b_i(0) = 0$, for $1 \leqslant i \leqslant p$.

THEOREM 1: *Under Conditions C1-C7, the functional estimator $\hat{\boldsymbol{\theta}}_n = \mathbb{Q}_n(\hat{F}_n)$ for the parameters in Model (1) is consistent and asymptotically normally distributed with a convergence rate of $n^{\frac{1}{2}}$, i.e., $\sqrt{n}(\hat{\boldsymbol{\theta}}_n - \boldsymbol{\theta}_0) \xrightarrow{D} N(\mathbf{0}, \boldsymbol{\Sigma})$, where $\boldsymbol{\theta}_0 = (\lambda_0, \alpha_0, \beta_0)^t$ is the true value of the parameter vector and*

$$\boldsymbol{\Sigma} = \left[E\left\{\boldsymbol{X}(F_0)^{\otimes 2}\right\}\right]^{-1} E\left[\left[\left\{\boldsymbol{\Phi}(U,V) + \boldsymbol{X}(F_0)^t \boldsymbol{A}\right\}^t\right]^{\otimes 2}\right]\left[E\left\{\boldsymbol{X}(F_0)^{\otimes 2}\right\}\right]^{-1},$$

where $\boldsymbol{\Phi}(U,V) = \big(0, \quad \phi_1(U,V), \quad \phi_2(U,V)\big)^t$,

$$\boldsymbol{X}(F_0) = \begin{pmatrix} \mathbf{Z}^t & E_{F_0, U<T\leqslant V}\boldsymbol{B}(U-T)^t & \mathbf{0} \\ \mathbf{Z}^t & \mathbf{0} & E_{F_0, U<T\leqslant V}\boldsymbol{B}(V-T)^t \end{pmatrix}$$

$$\boldsymbol{A} = \begin{pmatrix} \boldsymbol{\alpha}_0^t\Big\{\boldsymbol{B}(U-T) - E_{F_0,U<T\leqslant V}\boldsymbol{B}(U-T)\Big\} + \epsilon_U \\ \boldsymbol{\beta}_0^t\Big\{\boldsymbol{B}(V-T) - E_{F_0,U<T\leqslant V}\boldsymbol{B}(V-T)\Big\} + \epsilon_V \end{pmatrix}$$

and we denote $\boldsymbol{M}^t\boldsymbol{M}$ *as* $\boldsymbol{M}^{\otimes 2}$ *for any matrix* $\boldsymbol{M}$*. Functions* ϕ_1 *and* ϕ_2 *are the unique solutions to the following integral equations, respectively.*

$$\int\limits_{U<T\leqslant V} \phi_1(U,V)dH(U,V) = \int\limits_{U<T\leqslant V} \frac{\mathbf{B}(U-T)\Big\{F_0(V)-F_0(U)\Big\} - \int_U^V \mathbf{B}(U-s)dF_0(s)}{\Big\{F_0(V)-F_0(U)\Big\}^2} \cdot E_{F_0,U<s\leqslant V} Y_U dH(U,V|T),$$

$$\int\limits_{U<T\leqslant V} \phi_2(U,V)dH(U,V) = \int\limits_{U<T\leqslant V} \frac{\mathbf{B}(V-T)\Big\{F_0(V)-F_0(U)\Big\} - \int_U^V \mathbf{B}(V-s)dF_0(s)}{\Big\{F_0(V)-F_0(U)\Big\}^2} \cdot E_{F_0,U<s\leqslant V} Y_V dH(U,V|T),$$

where $H(U,V|T)$ *is the measure associated with the conditional joint distribution of* U *and* V*, given* $U < T \leqslant V$*.*

A few remarks are in order for the proof and the regularity conditions:

Remark 1 Essential details of the proof for the theorem are presented in Web Appendix A. Briefly, the proof is completed in two steps. First, we show that $\sqrt{n}(\tilde{\boldsymbol{\theta}}_n - \boldsymbol{\theta}_0)$ is asymptotically normal, where $\tilde{\boldsymbol{\theta}}_n = \mathbb{Q}_n(F_0)$ is the M-estimator of $\mathbb{M}_n(\boldsymbol{\theta}; F_0)$, i.e., the parameter estimate when the true distribution F_0 is known. Then, we examine the difference $\sqrt{n}(\hat{\boldsymbol{\theta}}_n - \tilde{\boldsymbol{\theta}}_n) = \sqrt{n}(\hat{\boldsymbol{\theta}}_n - \boldsymbol{\theta}_0) - \sqrt{n}(\tilde{\boldsymbol{\theta}}_n - \boldsymbol{\theta}_0)$, which is by definition $\sqrt{n}\Big\{\mathbb{Q}_n(\hat{F}_n) - \mathbb{Q}_n(F_0)\Big\}$. Using the empirical process theory, we show that this quantity times $E\Big\{\boldsymbol{X}(F_0)^{\otimes 2}\Big\}$ is asymptotically equivalent to $\sqrt{n}\big\{\boldsymbol{K}(\hat{F}_n) - \boldsymbol{K}(F_0)\big\}$, where $\boldsymbol{K}$ is an appropriately defined deterministic smooth functional. Using the general result from Geskus and Groeneboom (1999), we show that $\sqrt{n}\Big\{\boldsymbol{K}(\hat{F}_n) - \boldsymbol{K}(F_0)\Big\}$ has an asymptotic linear expansion. Combining the above steps, we establish the consistency and the asymptotic normality of $\hat{\boldsymbol{\theta}}_n$.

Remark 2: C1-C3 are the general regularity conditions needed to ensure consistency and convergence rate of $\hat{F}_n$ (Groeneboom and Wellner, 1992). Conditions C4-C6 are distributional

requirements for the observation and anchoring event times. These conditions are needed for studying the asymptotic properties of the class of functionals of $\hat{F}_n$ (Geskus and Groeneboom 1999), and thus helping in the derivation of the asymptotic normality of $\hat{\boldsymbol{\theta}}_n$. In most of the interval-censored data situations, these conditions are fairly mild and they pose no extra restrictions on the application. C7 is a regularity condition for $\boldsymbol{B}(t)$. We require $b_i(0) = 0$ to ensure that the function does not include another intercept term for the purpose of model identifiability, because the design matrix $\boldsymbol{Z}$ already has values 1 in its first column for the intercept.

Remark 3: Given its complicated structure, direct evaluation of the variance matrix $\boldsymbol{\Sigma}$ is difficult. Since the asymptotic normality is established and $\hat{\boldsymbol{\theta}}_n$ is relatively easy to compute, it is usually more convenient to use a resampling method to estimate $\boldsymbol{\Sigma}$. Here we estimate $\boldsymbol{\Sigma}$ by using a nonparametric bootstrap method. Specifically, for a data set containing n subjects, we draw bootstrap resamples containing n subjects from the original sample with equal weight and with replacement. We obtain a prespecified number ($b = 1, \ldots, B$) of resamples independently, from which we then calculate B estimates $\hat{\boldsymbol{\theta}}_n^{(b)}, b = 1, \ldots, B$. We use the sample variance matrix of these estimates $\hat{\boldsymbol{\theta}}_n^{(b)}, b = 1, \ldots, B$, to approximate $\boldsymbol{\Sigma}$; such a variance estimate is known to be consistent (Efron and Tibshirani, 1994).

4. Simulation study

To evaluate the operating characteristics of the proposed method, we conducted two sets of simulation studies.

4.1 *Data generation and simulation setup*

We designed the simulation to mimic the data generation process in the pubertal growth study: We first generated the "true" anchoring event times from a Weibull distribution, $T_i \sim$Weibull(80, 12). This distribution has a mean of $12 \cdot \Gamma(1+1/80) = 11.9$, which resembles

the pubertal growth spurt ages in girls between 11 and 12 years. We then simulated a series of visit times from an independent process; we considered two different visit frequencies, once every year or once every other year. The visit times were generated from Uniform$(j, j+1)$ or Uniform$(2j, 2j+2)$, $j = 0, 1, \cdots$, which respectively represented narrower and wider assessment intervals. From the generated visit times, we identified the two visits immediately before and after the anchoring event time T_i and use them as the boundaries of the censoring interval. In other words, U_i and V_i are the adjacent points selected from the series of the simulated assessment times that bracket the true anchoring event time T_i, i.e., $U_i < T_i \leqslant V_i$.

We then simulated the growth outcomes from the prespecified piece-wise linear model:

$$Y_{U_i} = \lambda + \alpha \cdot (U_i - T_i) + \epsilon_{U_i}, \quad Y_{V_i} = \lambda + \beta \cdot (V_i - T_i) + \epsilon_{V_i},$$

where $(\epsilon_{U_i}, \epsilon_{V_i})^t$ were simulated from the bivariate normal distribution $\boldsymbol{N}(\boldsymbol{\mu}, \boldsymbol{\Omega})$, with

$$\boldsymbol{\mu} = \begin{pmatrix} 0 \\ 0 \end{pmatrix}, \quad \boldsymbol{\Omega} = \begin{pmatrix} 5 & 4 \\ 4 & 5 \end{pmatrix}.$$

The true model parameters were chosen to be $\lambda = 50$, $\alpha = 5$ and $\beta = 8$. We considered four different sample sizes, $n = 100, 200, 400$ and 800. For a given sample size, we conducted a Monte-Carlo simulation with 1000 replicates.

For each simulated data set, we performed four different analyses. First, we fitted the model with the proposed two-step procedure. Second, we fitted the model with a midpoint imputation for the unobserved T_i, i.e., imputing T_i with the midpoint of the interval $(U_i, V_i]$, and then estimated the parameters using the ordinary least-squares method. Mid-point imputation is a naive method but it is a commonly used technique in analytical practice (Shankar et al., 2005). The third method we tested was a model assuming the true anchoring event times F_0 follows a normal distribution with unknown mean μ and variance σ^2. The parameters $(\lambda, \alpha, \beta; \mu, \sigma^2)$ were jointly estimated as described by van den Hout et al., (2013). Finally, we fitted the model assuming the true anchoring event time distribution F_0 was

known, i.e., we used F_0 instead of $\hat{F}_n$ in Step 2 to obtain parameter estimates. The final scenario, of course, is not realistic for our application; we simply used it to establish a benchmark to investigate the efficiency loss due to the estimation of F_0. The estimated standard errors for these four methods were obtained by using the previously described bootstrap method, based on $B = 50$ resamples.

For 1000 replicates of samples of size n, we reported the percentages of average estimation bias, Monte-Carlo standard deviations, average bootstrap standard errors, and the empirical coverage probabilities of the 95% Wald confidence intervals based on the asymptotical normality described in Theorem 1.

4.2 *Simulation results*

We summarized simulation results for parameter estimates for all methods in a tabular form. Results for wider and narrower assessment intervals are presented in Tables 1 and 2.

[Table 1 about here.]

[Table 2 about here.]

Tables 1 and 2 showed that the estimation bias in the proposed method was virtually ignorable, even at the moderate sample size of $n = 100$. The average bootstrap standard errors were all close to the corresponding Monte-Carlo standard deviations. In addition, the coverage probabilities of the 95% Wald confidence intervals approached the nominal level of 0.95 as the sample size increased. In summary, the simulation has provided strong numerical evidence in support of the asymptotic normality theory developed in Section 3.

In comparison, the estimation bias in the midpoint imputation method was much larger. The magnitude of the bias did not reduce with an increasing sample size. Both the Monte-Carlo standard deviations and bootstrap standard errors of the midpoint imputation were also markedly larger than those in the proposed method. The 95% Wald confidence intervals

from the midpoint imputation method actually had decreasing coverage probabilities when the sample size increased. In comparison with the normal models, (van den Hout et al, 2013) the proposed method tended to produce estimates with smaller bias and variance estimates, due to its increased robustness. As one would expect, parameter estimation performed best in the hypothetical situation of known F_0.

It is important to note that the variance estimates from the proposed method were only slightly larger than those obtained under F_0. To empirically evaluate the relative efficiency, we calculated the ratio of the Monte-Carlo standard deviations and average bootstrap standard errors in the proposed model over those of known F_0; see Table 3. All ratios were generally close to 1, especially for the local change rates α and β, the main parameters of interesting, suggesting no significant efficiency loss.

[Table 3 about here.]

In summary, the simulation study provides strong empirical evidence in support of a good finite sample performance of the proposed method.

5. Analysis of skeletal growth data

For illustration, we analyzed the pubertal growth data from 360 children. The original data came from an observational study of somatic growth and blood pressure development. The study protocol was described elsewhere (Tu et al., 2009, 2014). In the current analysis, we aimed at determining the rates of skeletal growth in height, upper body length (i.e., height in sitting position), shoulder length, elbow, wrist, and knee diameters, and to compare the rates between male and female participants, immediately before and after the subject-specific PGS.

Although the exact PGS time for an individual was not observable, the investigators were able to determine the assessment times that flanked the unobserved PGS (Shankar et al.,

2005), which we referred to as the peak growth periods. The current analysis included a total of 169 girls and 191 boys. The age range from the youngest and the oldest assessment times was between 9.005 and 16.930 years, thus ensuring the coverage of PGS in all participants. Figure 1 shows the peak growth intervals for the study children. The doted vertical lines represent the estimated median PGS times for girls and boys. Given the skeletal measurements at the endpoints of these intervals, we used the proposed method to estimate the change rates in these outcomes before and after the unobserved PGS.

[Figure 1 about here.]

The skeletal measures of interest, including height, upper body length, shoulder length, elbow, wrist and knee diameters of the participants in the peak growth intervals are shown in Figure 2, stratified by sex. The figure clearly showed that significant changes occurred simultaneously in all skeletal dimensions during the peak growth period.

[Figure 2 about here.]

As proposed, we used the NPMLE of the unknown CDF to depict the PGS time distribution in male and female children, as shown in Figure 3. From the NPMLE of the CDFs, we estimated the median ages of PGS to be 11.05 years for girls, and 12.74 years for boys.

[Figure 3 about here.]

We fitted a simple piece-wise model $E(Y_U) = \lambda + \alpha \cdot (U - T)$ and $E(Y_V) = \lambda + \beta \cdot (V - T)$ separately for boys and girls, where Y_U and Y_V were the observed values of the skeletal variables, including height, upper body length, shoulder length, and elbow, wrist, and knee diameters, measured at the two endpoints of $(U, V]$, respectively. As previously stated, we limited the current analysis to the estimation of skeletal change rates around PGS, so we did not consider inclusion of data that were outside the peak growth interval; the measures

collected at more remote time points were not informative of the local behaviors that we tried to depict.

The functional estimates of the pre and post-PGS skeletal growth in the six measures, stratified by sex, are presented graphically in Figure 4.

[Figure 4 about here.]

Inference on the post-PGS growth rate changes from the pre-PGS period can be made based on the asymptotic results of Theorem 1. Depending the specific need of testing, one could express hypotheses in the form of a linear contrast $\mathbf{e}^t\boldsymbol{\theta}$, and then test $H_0: \quad \mathbf{e}^t\boldsymbol{\theta} = 0$. This two-sided test statistic, therefore, takes the form $n(\mathbf{e}^t\hat{\boldsymbol{\Sigma}}_n\mathbf{e})^{-1}\left(\mathbf{e}^t\hat{\boldsymbol{\theta}}_n\right)^2$, where $\hat{\boldsymbol{\theta}}_n$ is the parameter estimate and $\hat{\boldsymbol{\Sigma}}_n$ is the bootstrap estimate of the asymptotic variance. The test statistic followed a χ^2-distribution with 1 degree of freedom asymptotically according to Theorem 1. For example, setting $\mathbf{e} = (0, -1, 1)^t$, one could compare the pre-PGS rate α with the post-PGS rate β of a specified outcome.

Similarly, one could make inference on the difference of the post-PGS growth rates between boys and girls by testing hypothesis $H_0: \ \mathbf{e}^t(\boldsymbol{\theta_1} - \boldsymbol{\theta_2}) = 0$. The corresponding test statistic can be derived from the standard independent two-sample test given by

$$\left\{n_1^{-1}\left(\mathbf{e}^t\hat{\boldsymbol{\Sigma}}_{1,n_1}\mathbf{e}\right) + n_2^{-1}\left(\mathbf{e}^t\hat{\boldsymbol{\Sigma}}_{2,n_2}\mathbf{e}\right)\right\}^{-1}\left\{\mathbf{e}^t\left(\hat{\boldsymbol{\theta}}_{1,n_1} - \hat{\boldsymbol{\theta}}_{2,n_2}\right)\right\}^2$$

with $\mathbf{e} = (0, 0, 1)^t$, where $\hat{\boldsymbol{\theta}}_{1,n_1}$ and $\hat{\boldsymbol{\theta}}_{2,n_2}$ are the parameter estimates, and $\hat{\boldsymbol{\Sigma}}_{1,n_1}$ and $\hat{\boldsymbol{\Sigma}}_{2,n_2}$ are the bootstrap estimates of the asymptotic variances for the respective groups. Again, the test statistic follows a χ^2-distribution with 1 degree of freedom asymptotically.

This analysis represented the first attempt in quantifying the skeletal growth rates in boys and girls around the time of the PGS (See Figure 4). The analysis clearly showed that boys and girls experienced different rates of skeletal growth around the PGS. Three important observations emerged from the analysis: (1) Skeletal growth continued at the PGS in both sexes, as shown by the strictly positive growth rates in all variables. (2) In comparison with

girls, boys had greater values in point estimates of the skeletal measures at the time of PGS (all p values less than 0.01). Interestingly, sex differences showed not only in the length of the bones but also in the thickness of the bones, in both pre and post-PGS periods. For example, in the post-PGS period, boy's elbow diameter increased at a rate of 0.57cm/year, significantly greater than girl's 0.28cm/year ($p = 0.03$). During the same period, boy's wrist diameter increased at a rate of 0.43cm/year, significantly greater than girl's 0.21cm/year ($p = 0.01$). (3) Boy's post-PGS growth rates were generally greater than their pre-PGS rates. The growth rate of upper-body length in boys increased from 2.64cm/year in the pre-PGS period to 5.68cm/year in the post-PGS period, a net increase of 3.04cm/year ($p = 0.02$), comparing to a slight decrease in girls from 4.02cm/year pre-PGS to 3.87cm/year post-PGS ($p = 0.88$). The same was true for the bone thickness. For example, the wrist diameter growth rate in boys increased from 0.17cm/year pre-PGS to 0.43cm/year post-PGS ($p = 0.04$).

When we considered all of six skeletal outcomes, the analysis provided a clear picture of the emergence of sexual dimorphism in human skeletal development. Although girls start puberty and reach their peak height growth velocity nearly two years earlier than boys, at the time of PGS, boys exceeded girls in all skeletal measures including both bone lengths and bone thickness. Importantly, boy's greater post-PGS growth rates in different body parts set the stage for a stronger and more sustained growth that ultimately led to their bigger average body size.

The findings, however, also raised intriguing questions about the regulation of such coordinated patterns of growth. One might speculate, for example, that sex differences around the PGS could be the result of a surging influence of androgenic hormones such as testosterone. In the absence of direct evidence, we note the simultaneous emergence of accelerated bone growth and male sexual characteristics right after PGS appears to give credence to such a speculation. Of course, variations in the timing, as well as in the duration of pubertal

growth, may suggest the existence of multiple operators, including hormonal (Rose et al., 1991), nutritional (Whiting et al., 2004), and genetic (Tu et al., 2015) influences on the rapid skeletal development in puberty.

For a comparison purpose, we also fitted the piece-wise linear model using midpoint imputation and normally distributed PGS time, as discussed in Section 4. The parameter estimates and standard errors of these two models and our proposed model were summarized in the following table. The standard errors for the three models were obtained using the same 200 bootstrap samples.

[Table 4 about here.]

Table 4 showed that midpoint imputation did not generate reasonable estimates. For instance, negative growth rates should not happen near the PGS. The model based on parametric normal distribution also yielded unexpected estimates. In boys, for example, the parametric model produced a drastically lower post-PGS height growth rate, as compared to the pre-PGS rate. Such an estimate is inconsistent with the general knowledge that boys maintain vigorous height growth after the PGS, till they approach their adult heights. An important point that should not be lost in discussion is that the validity of parametric analysis always depends on the correct specification of the underlying distribution, which in the current application is difficult to verify.

6. Discussion

Estimation of local change rates around unobserved anchoring events is a frequently encountered issue in scientific investigation. Appropriate analytical methodology, however, has not been forthcoming. Considering the essential roles that anchoring events play in the analysis, it is surprising that this issue has not received more attention in the existing literature. How the unobserved anchoring points influence analysis and how they should be handled

in practice are questions that remain unsettled. Although *ad hoc* methods abound, careful methodological development and rigorous theoretical justification are virtually nonexistent. To the best of our knowledge, this is the first rigorous study of these issues.

By framing the question in the context of least squares models, we sought to estimate model parameters without resorting to imputing the subject-specific anchoring times or imposing parametric distributions for the unobserved events. We demonstrated that by using an estimated anchoring event time distribution, one could completely sidestep the imputation and parametric formulation to achieve valid estimation and inference. We showed that the resultant functional estimators are in possession of the desired convergence rate of $\sqrt{n}$ and asymptotic normal distribution.

Importantly, the method makes no parametric assumptions for the anchoring event time and the error terms. As long as the model is correctly specified and the regularity conditions are met, the parameter estimators will be consistent and asymptotically normally distributed, so large sample inference could proceed without difficulty. Our simulation study confirmed the performance of the method in finite sample situations. The magnitudes of the biases, for example, were almost negligible in comparison with the magnitudes of the actual effects. The coverage probabilities of the confidence intervals were also close to the nominal level.

In practice, applying the method requires reliable identification of the intervals within which the anchoring events reside. As we have demonstrated in the simulation study, good estimation and inference performance can be achieved as long as the censoring intervals are correctly specified. In real applications, identification of the censoring intervals is likely to depend on the specifics of the study setting. In the present example, we have determined the censoring intervals by comparing the growth rates between the adjacent visits. In other applications, determination of censoring intervals may depend on the specific disease screening practice or even on experts' clinical judgment. In either case, incorrectly specified

censoring intervals represent a source of misclassification. The impact of misclassification can be examined through carefully designed sensitivity analyses. A related restriction is that we assume the process producing the censoring intervals to be independent of the true anchoring event distribution. While such an assumption is reasonable in our example, there may be situations where it is less defendable. In those circumstances, incorporating the correlations between the anchoring event times and the visit times becomes necessary for the estimation of F_0. We are currently studying this issue.

This work represents an important step towards sorting out the methodological issues concerning the unobserved anchoring events. This distribution-free approach has allowed us to operate with virtually no distributional constraints and thus is quite robust against model misspecification. To some extent, the robustness may have been gained at the expense of estimation efficiency. But if our simulation study is of any guidance, the efficiency loss appears to be rather minimal.

In a practical data analysis, one should always weigh the pros and cons of parametric vs. nonparametric methods. In some situations, parametric methods have a greater capacity to accommodate the more complex modeling structures. In this analysis, we have primarily focused on the estimation of the *population-average* skeletal growth rates. The method has a certain affinity to the generalized estimating equations (GEE) models. In our application, we did not attempt to accommodate the individual-specific growth rates. Had that been an interest, one would have to consider incorporating random slopes into the model, and thus necessitating parametric assumptions. That extension goes beyond the scope of distribution-free estimation and requires different theoretical justifications. The fundamental idea of the two-step procedure, however, remains relevant.

Scientifically, the research has generated valuable insights that the traditional analysis fails to provide. By quantifying the skeletal growth rates before and after the PGS, we showed

that the sex differences in adult bodies started to emerge before the PGS and continued after it. In particular, the maintenance of the post-PGS skeletal growth rates in boys, in multiple body parts, appears to be a main driving force for the sexual dimorphism in human growth. This, among other things, strongly implicates gonadal hormones' influences on pubertal development.

7. Supplementary Materials

Web Appendix A, referenced in Section 3, is available at the *Biometrics* website in Wiley Online Library. Example data and computational code are also included as parts of the supplementary materials.

Acknowledgements

This research is supported by NIH grants HL095086 and AA025208. The authors are grateful to the Associate Editor and two anonymous reviewers for their excellent comments. Their insights have helped us improve the quality of the manuscript.

References

Carter, C. L., Allen, C., and Henson, D. E. (1989). Relation of tumor size, lymph node status, and survival in 24,740 breast cancer cases. *Cancer* **63,** 181–187.

Efron, B., and Tibshirani, R. J. (1994). *An introduction to the bootstrap*. Boca Raton: CRC press.

Fournier, D., Weber, E., Hoeffken, W., Bauer, M., Kubli, F., and Barth, V. (1980). Growth rate of 147 mammary carcinomas. *Cancer* **45,** 2198–2207.

Gasser, T., Muller, H. G., Kohler, W., Molinari, L., and Prader. A. (1984). Nonparametric regression analysis of growth curves. *The Annals of Statistics* **12,** 210–229.

Geskus, R., and Groeneboom. P. (1999). Asymptotically optimal estimation of smooth functionals for interval censoring, case 2. *The Annals of Statistics* **27,** 627–674.

Groeneboom, P., and Wellner, J. A. (1992). *Information bounds and nonparametric maximum likelihood estimation, volume 19*. Springer Science & Business Media.

Huber, P. J. (2011). *Robust statistics*. Berlin Heidelberg:Springer.

Kosorok, M. R. (2008). *Introduction to empirical processes and semiparametric inference*. New York:Springer.

Lee., T.S. (2010). Change-point problems: bibliography and review. *Journal of Statistical Theory and Practice* **4,** 643–662.

Preece, M., and Baines, M. (1978). A new family of mathematical models describing the human growth curve. *Annals of human biology* **5,** 1–24.

Robinson, L. F., Wager, T. D., and Lindquist, M. A. (2010). Change point estimation in multisubject fmri studies. *Neuroimage* **49,** 1581–1592.

Rose, S. R., Municchi, G., Barnes, K. M., Kamp, G. A., Uriate, M. M., Ross, J. L., et al. (1991). Spontaneous growth hormone secretion increases during puberty in normal girls and boys. *The Journal of Clinical Endocrinology & Metabolism* **73,** 428–435.

Shankar, R. R., Eckert, G. J., Saha, C., Tu, W., and Pratt, J. H. (2005). The change in blood pressure during pubertal growth. *The Journal of Clinical Endocrinology & Metabolism* **90,** 163–167.

Spratt, J. A., Fournier, D. Von, Spratt, J. S., and Weber, E. E. (1993). Decelerating growth and human breast cancer. *Cancer* **71,** 2013–2019.

Tanner, J. M., and Whitehouse, R. H. (1976). Clinical longitudinal standards for height, weight, height velocity, weight velocity, and stages of puberty. *Archives of disease in childhood* **51,** 170–179.

Tu, W., Eckert, G. J., Saha, C., and Pratt, J. H. (2009). Synchronization of adolescent blood pressure and pubertal somatic growth. *The Journal of Clinical Endocrinology & Metabolism* **94,** 5019–5022.

Tu, W., Eckert, G. J., Hannon, T. S., Liu, H., Pratt, L. M., Wagner, M. A., et al. (2014). Racial differences in sensitivity of blood pressure to aldosterone. *Hypertension* **63,** 1212–1218.

Tu, W., Wagner, E. K., Eckert, G. J., Yu, Z., Hannon, T., Pratt, J. H., el al. (2015). Associations between menarche-related genetic variants and pubertal growth in male and female adolescents. *Journal of Adolescent Health* **56,** 66–72.

van den Hout, A., Muniz-Terrera,G., and Matthews., F. E. (2013) Change point models for cognitive tests using semi-parametric maximum likelihood. *Computational statistics & data analysis* **57,**684–698.

Whiting, S. J., Vatanparast, H., Baxter-Jones, A., Faulkner, R. A., Mirwald, R., and Bailey, D. A. (2004). Factors that affect bone mineral accrual in the adolescent growth spurt. *The Journal of nutrition* **134,** 696–700.

Zhang, Y., and Jamshidian, M. (2004). On algorithms for the nonparametric maximum likelihood estimator of the failure function with censored data. *Journal of Computational*

and Graphical Statistics **13,** 123–140.

Zhang, Y., Cheng, G., and Tu, W. (2016). Robust nonparametric estimation of monotone regression functions with interval-censored observations. *Biometrics* **72,** 720-730.

Zhang, Z., and Sun, J. (2010). Interval censoring. *Statistical Methods in Medical Research* **19,** 53–70.

Figure 1. Peak growth periods in 360 children

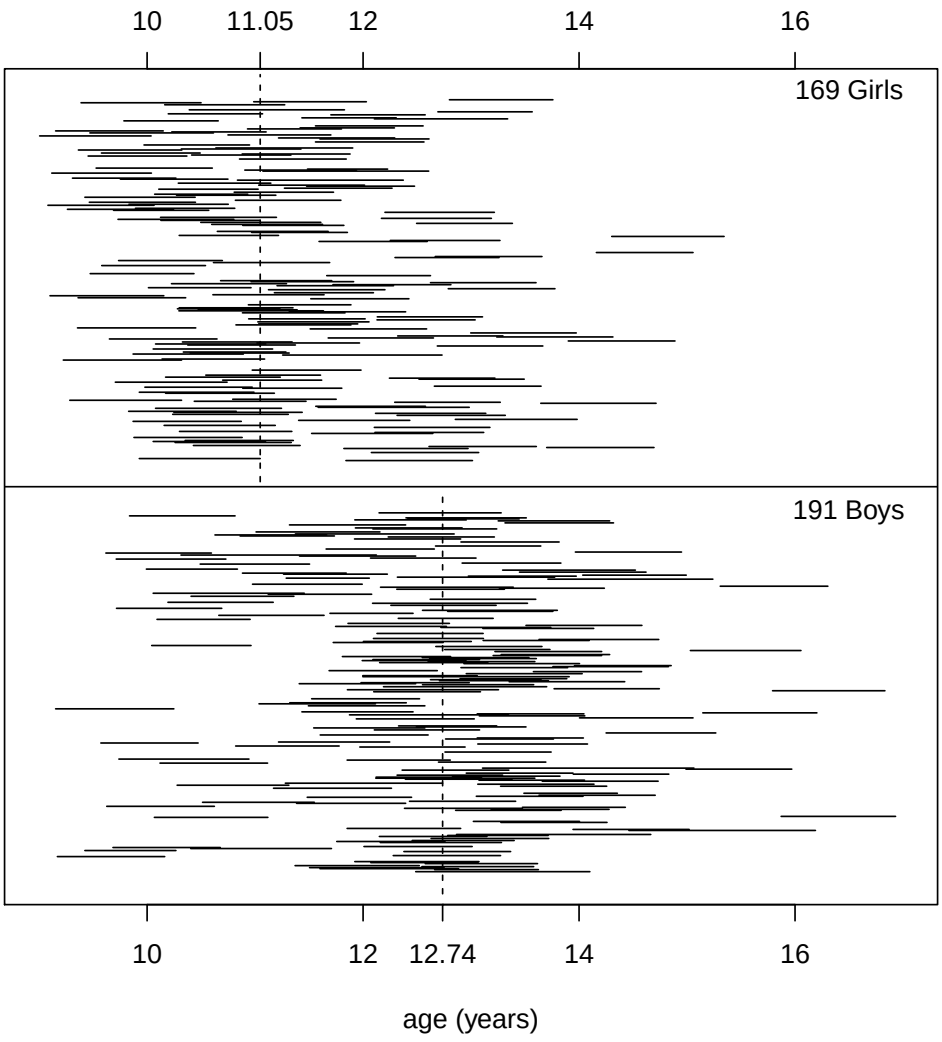

Figure 2. Skeletal measurements in the peak growth intervals. This figure appears in color in the electronic version of this article.

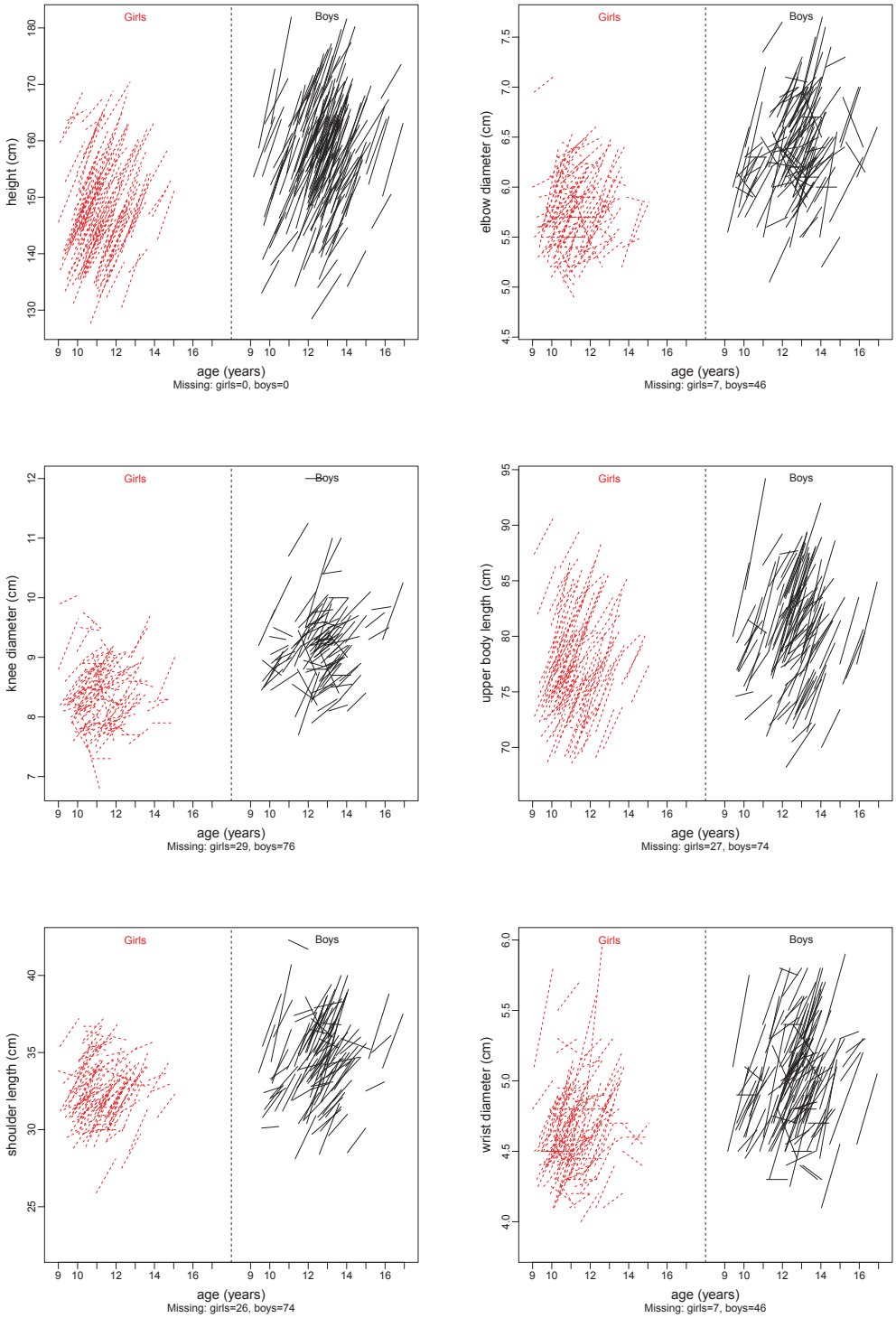

Figure 3. The estimated CDFs of F_0 for males and females. This figure appears in color in the electronic version of this article.

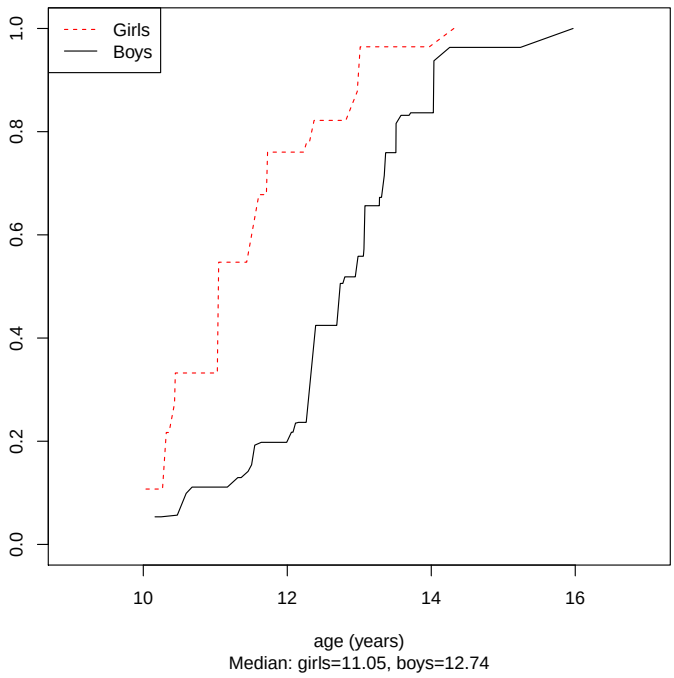

Figure 4. The fitted anchoring point models. This figure appears in color in the electronic version of this article.

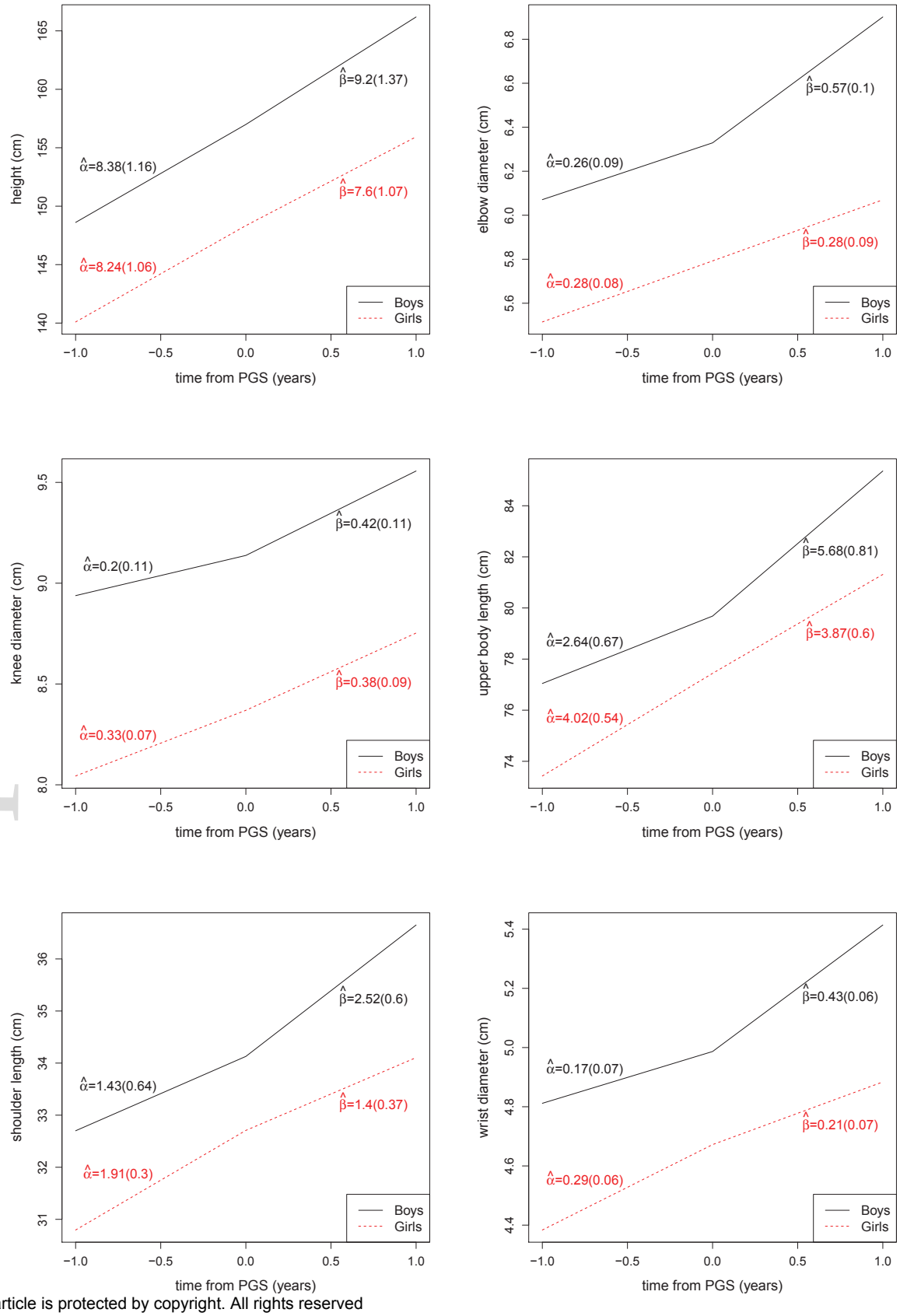

Table 1

Simulation results for wider censoring intervals. % Bias: Percentage of average bias; M-C SD: Monte-Carlo standard deviation; Av. SE: Average estimated standard error; 95% CP: Empirical coverage probability of the estimated 95% Wald confidence interval.

	$\lambda = 50$				$\alpha = 5$				$\beta = 8$			
n	100	200	400	800	100	200	400	800	100	200	400	800
Proposed model:												
% Bias	0.182	0.052	0.047	0.017	0.117	0.464	0.115	0.189	0.417	0.212	0.240	0.178
M-C SD	0.453	0.291	0.215	0.147	0.254	0.173	0.128	0.086	0.278	0.193	0.137	0.094
Av. SE	0.425	0.297	0.207	0.146	0.244	0.175	0.124	0.088	0.274	0.192	0.134	0.096
95% CP	0.916	0.944	0.937	0.945	0.939	0.938	0.942	0.948	0.942	0.949	0.939	0.951
Midpoint imputation:												
% Bias	1.195	1.135	1.223	1.160	11.022	10.512	11.034	10.587	7.237	7.005	7.217	7.035
M-C SD	1.041	0.748	0.530	0.360	1.023	0.710	0.508	0.350	1.139	0.774	0.556	0.388
Av. SE	1.031	0.738	0.521	0.371	0.987	0.710	0.504	0.359	1.086	0.782	0.556	0.396
95% CP	0.915	0.870	0.789	0.655	0.907	0.879	0.804	0.682	0.904	0.883	0.818	0.699
Normal distribution assumption:												
% Bias	0.463	0.255	0.245	0.223	0.170	0.361	0.167	0.345	1.723	1.267	0.978	0.910
M-C SD	0.792	0.568	0.398	0.269	0.261	0.184	0.129	0.088	0.342	0.238	0.169	0.112
Av. SE	0.738	0.555	0.394	0.278	0.257	0.183	0.129	0.090	0.380	0.251	0.172	0.120
95% CP	0.912	0.926	0.941	0.942	0.942	0.944	0.945	0.957	0.964	0.951	0.931	0.930
Use true F_0:												
% Bias	0.018	0.022	0.006	0.006	0.226	0.121	0.130	0.028	0.013	0.114	0.015	0.006
M-C SD	0.354	0.245	0.177	0.119	0.257	0.176	0.126	0.085	0.277	0.190	0.134	0.092
Av. SE	0.343	0.245	0.172	0.121	0.252	0.178	0.125	0.087	0.269	0.190	0.132	0.094
95% CP	0.947	0.948	0.932	0.944	0.948	0.947	0.944	0.953	0.940	0.949	0.933	0.957

Table 2

Simulation results for narrower censoring intervals. % Bias: Percentage of average bias; M-C SD: Monte-Carlo standard deviation; Av. SE: Average estimated standard error; 95% CP: Empirical coverage probability of the estimated 95% Wald confidence interval.

	$\lambda = 50$				$\alpha = 5$				$\beta = 8$			
n	100	200	400	800	100	200	400	800	100	200	400	800
Proposed model:												
% Bias	0.123	0.050	0.053	0.028	0.118	0.646	0.013	0.094	1.446	0.880	0.786	0.536
M-C SD	0.367	0.241	0.185	0.123	0.456	0.331	0.238	0.161	0.499	0.346	0.247	0.166
Av. SE	0.346	0.248	0.175	0.124	0.434	0.316	0.228	0.162	0.482	0.343	0.243	0.174
95% CP	0.932	0.951	0.931	0.947	0.945	0.937	0.939	0.945	0.925	0.935	0.936	0.952
Midpoint imputation:												
% Bias	0.500	0.446	0.521	0.487	9.143	7.920	9.089	8.510	5.929	5.204	5.880	5.615
M-C SD	0.807	0.589	0.420	0.274	1.479	1.077	0.763	0.500	1.578	1.139	0.810	0.532
Av. SE	0.810	0.578	0.405	0.289	1.470	1.044	0.735	0.527	1.566	1.112	0.783	0.563
95% CP	0.936	0.925	0.895	0.870	0.932	0.922	0.896	0.875	0.924	0.925	0.899	0.872
Normal distribution assumption:												
% Bias	0.416	0.243	0.258	0.235	0.565	1.349	0.827	1.056	4.296	3.228	2.678	2.569
M-C SD	0.648	0.437	0.315	0.208	0.462	0.328	0.229	0.153	0.676	0.457	0.328	0.212
Av. SE	0.609	0.446	0.316	0.219	0.479	0.331	0.229	0.160	0.816	0.484	0.319	0.221
95% CP	0.917	0.933	0.930	0.946	0.957	0.952	0.945	0.940	0.965	0.938	0.910	0.876
Use true F_0:												
% Bias	0.006	0.023	0.005	0.001	0.348	0.342	0.201	0.035	0.073	0.177	0.032	0.016
M-C SD	0.344	0.232	0.174	0.114	0.479	0.338	0.241	0.160	0.515	0.343	0.248	0.166
Av. SE	0.331	0.237	0.166	0.117	0.470	0.331	0.234	0.164	0.497	0.350	0.244	0.173
95% CP	0.935	0.954	0.939	0.956	0.947	0.942	0.946	0.953	0.940	0.943	0.939	0.959

Table 3

Empirical relative efficiency of the proposed method vs the case of known F_0. M-C SD: Ratio of Monte-Carlo standard deviations; Av. SE: Ratio of the average estimated standard errors.

	$\lambda = 50$				$\alpha = 5$				$\beta = 8$			
n	100	200	400	800	100	200	400	800	100	200	400	800
Wider censoring intervals												
M-C SD	1.280	1.191	1.213	1.233	0.986	0.986	1.008	1.013	1.005	1.016	1.019	1.023
Av. SE	1.238	1.209	1.205	1.203	0.967	0.985	0.996	1.005	1.019	1.013	1.015	1.021
Narrower censoring intervals												
M-C SD	1.068	1.038	1.060	1.082	0.952	0.978	0.989	1.007	0.969	1.007	0.992	1.000
Av. SE	1.047	1.047	1.052	1.057	0.924	0.953	0.975	0.988	0.970	0.981	0.994	1.004

Table 4

Estimates of pubertal growth parameters from three models. Model I: The proposed model; Model II: The midpoint imputation model; Model III: A model based on normal distribution approximation. Unit for $\hat{\lambda}$: cm; unit for $\hat{\alpha}$ and $\hat{\beta}$:cm/year.

Variable	Model	Boys			Girls		
		$\hat{\lambda}$ (*se*)	$\hat{\alpha}$ (*se*)	$\hat{\beta}$ (*se*)	$\hat{\lambda}$ (*se*)	$\hat{\alpha}$ (*se*)	$\hat{\beta}$ (*se*)
Height	I	156.99 (0.97)	8.38 (1.16)	9.20 (1.37)	148.34 (0.71)	8.24 (1.06)	7.60 (1.07)
	II	155.13 (3.73)	4.79 (6.73)	12.37 (6.77)	148.63 (5.41)	8.48 (10.68)	6.45(10.67)
	III	156.39 (0.79)	13.36 (1.79)	8.64 (0.66)	149.08 (0.68)	9.85 (0.83)	8.65 (0.94)
Elbow diameter	I	6.33 (0.06)	0.26 (0.09)	0.57 (0.10)	5.79 (0.05)	0.28 (0.08)	0.28 (0.09)
	II	6.10 (0.24)	-0.19 (0.45)	0.95 (0.45)	5.64 (0.45)	-0.02 (0.89)	0.57 (0.89)
	III	6.32 (0.05)	0.46 (0.07)	0.47 (0.05)	5.77 (0.30)	0.31 (0.69)	0.27 (0.65)
knee diameter	I	9.14 (0.08)	0.20 (0.11)	0.42 (0.11)	8.37 (0.05)	0.33 (0.07)	0.38 (0.09)
	II	8.69 (0.54)	-0.64 (1.03)	1.32 (1.05)	7.96 (0.74)	-0.50 (1.47)	1.15 (1.47)
	III	9.13 (0.11)	0.54 (0.24)	0.39 (0.25)	8.38 (0.17)	0.42 (0.37)	0.33 (0.29)
Shoulder length	I	34.13 (0.39)	1.43 (0.64)	2.52 (0.60)	32.71 (0.19)	1.91 (0.30)	1.40 (0.37)
	II	31.23 (1.67)	-4.05 (3.02)	8.287 (3.08)	35.09 (2.63)	6.71 (5.27)	-3.52 (5.28)
	III	33.93 (0.28)	2.58 (0.91)	2.51 (0.26)	32.66 (0.17)	1.82 (0.18)	2.18 (0.30)
Upper body length	I	79.68 (0.54)	2.64 (0.67)	5.68 (0.81)	77.44 (0.41)	4.02 (0.54)	3.87 (0.60)
	II	74.53 (3.24)	-7.56 (6.12)	15.46 (6.10)	81.26 (4.71)	11.61 (9.30)	-4.14 (9.28)
	III	79.61 (0.43)	4.22 (0.66)	4.96 (0.39)	77.69 (0.40)	4.83 (0.35)	4.66 (0.54)
Wrist diameter	I	4.99 (0.05)	0.17 (0.07)	0.43 (0.06)	4.67 (0.04)	0.29 (0.06)	0.21 (0.07)
	II	4.82 (0.17)	-0.14 (0.31)	0.74 (0.31)	4.95 (0.30)	0.82 (0.59)	-0.34 (0.59)
	III	4.97 (0.07)	0.32 (0.14)	0.33 (0.19)	4.64 (0.20)	0.28 (0.54)	0.26 (0.36)